Quaternary Geochronology 83 (2024) 101563

Contents lists available at ScienceDirect

Quaternary Geochronology

journal homepage: www.elsevier.com/locate/quageo

Research paper

Dating post-LGM aeolian sedimentation and the Late Palaeolithic in Central Yakutia (northeastern Siberia)

Mariya S. Lukyanycheva [a,*], Redzhep N. Kurbanov [b], Natalia A. Taratunina [c], Anzhela N. Vasilieva [d], Vasiliy M. Lytkin [e], Andrei V. Panin [b], Anton A. Anoikin [f], Thomas Stevens [g,h], Andrew S. Murray [i,c], Jan-Pieter Buylaert [c], Mads F. Knudsen [j]

[a] Institute of Archaeology and Anthropology, Azerbaijan National Academy of Sciences, Baku, Azerbaijan
[b] Institute of Water Problems, Hydropower and Ecology, NAST, Dushanbe, Tajikistan
[c] Department of Physics, Technical University of Denmark, Roskilde, Denmark
[d] Al-Farabi Kazakh National University, Almaty, Kazakhstan
[e] Institute of Geography and Water Security, Almaty, Kazakhstan
[f] National Museum of Kazakhstan, Astana, Kazakhstan
[g] Department of Geosciences, Uppsala University, Uppsala, Sweden
[h] Department of Geosciences and Geography, University of Helsinki, Helsinki, Finland
[i] Nordic Laboratory for Luminescence Dating, Department of Geoscience, University of Aarhus, Aarhus C, Denmark
[j] Department of Geoscience, Aarhus University, Aarhus C, Denmark

ARTICLE INFO

Keywords:
Aeolian deposits
Late Pleistocene climate
Lena river
OSL chronology
Late paleolithic archeology

ABSTRACT

Central Yakutia is a large region in northeastern Siberia characterized by extensive permafrost, large river valleys, mountain glaciers, and large massifs of aeolian sands; the geological history of the region is complex and, at present, poorly constrained. In recent years, it has been shown that aeolian sands cover up to 60% of large parts of Central Yakutia. This paper presents the results of luminescence dating of aeolian sedimentation at the Diring Yuriakh Palaeolithic site located in the middle reaches of the Lena River. Field studies identified several thick units of aeolian sand, which cover an old deflation surface with Late (Duktai culture) and Early Palaeolithic (Diring culture) artefacts. The reliability of the OSL chronology was assessed by comparison of ages based on the optically stimulated luminescence from quartz and the infra-red stimulated luminescence from potassium-rich feldspars; these age pairs are in good agreement, implying that at least the quartz grains were sufficiently bleached before sedimentation. We obtained OSL ages that reflect three periods of accumulation between the LGM and the Holocene: ~21 ka, 15-14 ka, and 12.5–10 ka. These periods of accumulation broadly coincide with global cooling episodes during the Last Glacial Maximum, the Older Dryas, and the Younger Dryas, with some extension into subsequent warmer intervals, whereas the intervening intervals without preserved sediments are taken to reflect dune stability during warmer periods. The sand on the terraces, sourced from alluvial bars in the river channel, was blown up the valley slope during cold and dry periods when the vegetation cover was sparse. When the climate warmed, the vegetation took some time to spread, and so the accumulation of aeolian sand on the high terraces continued into the warm periods. We also infer periods of deflation (wind erosion) that occurred before 21 ka and between 20 and 15 ka, presumably due to increased aeolian activity and localized remobilization of sediment. The new OSL chronology shows that the younger artefacts located at the cape of Diring Yuriakh, belonging to the Late Palaeolithic Duktai culture, are older than 15 ka. The new ages also show that the post-LGM aeolian sand sequences at Diring Yuriakh are correlated with the regionally developed sub-aerial Dolkuma Formation.

* Corresponding author.
E-mail address: mashluk95@gmail.com (M.S. Lukyanycheva).

https://doi.org/10.1016/j.quageo.2024.101563
Received 15 November 2023; Received in revised form 18 April 2024; Accepted 10 June 2024
Available online 25 June 2024

1. Introduction

Central Yakutia in northeastern Eurasia (Fig. 1) has an ultra-continental climate, making it one of the coldest areas on the planet. Very little is known of the Quaternary history of this remote region, many parts of which are difficult to access even today. The region covers the broad mountainous area of northeastern Siberia (Verkhoyanskiy and Cherskiy Ranges, Suntar-Khayata, Lena and Yana Upplands), numerous wide river valleys (Lena River and its large tributaries Aldan, Vitim, Viluy, Olekma, Yana, Kolyma, Indigirka) and extensive areas of permafrost. Yakutia provides the opportunity to study important climate archives, such as the glacial moraine series in the mountains, alluvial sediment in complex river terrace systems, and ice-rich permafrost loess (Yedoma formation). Currently, increasing attention is focused on climate change and landscape evolution in the Arctic, and this has increased interest in the palaeogeographic archives of Yakutia (Zech et al., 2011; Barr and Clark, 2012; Galanin, 2021), because of the sensitivity of high-latitude regions to climate change, and the global implications of this change e.g. via permafrost thawing. The topography and diversity of the Quaternary sediments indicate that the region experienced a complex climatic and environmental history. While new data are now available on the Quaternary evolution of the Lena River (Schirrmeister et al., 2011; Schwamborn et al., 2023), other areas have received much less attention; these include the glacial history of the adjacent mountains (Siegert et al., 2007; Nørgaard et al., 2023; Arzhannikov et al., 2024), Yedoma formation (Schirrmeister et al., 2013; Kuznetsova et al., 2022), and the aeolian sand landscapes of Central Yakutia.

Large parts of Yakutia are covered with aeolian sands and systems of aeolian ridges and dunes, which sometimes coalesce into sand seas. These deposits are up to 15–25 m thick and occupy up to 60% of the area of large regions of Central Yakutia (Galanin and Pavlova, 2019). After more than a century of study, a number of hypotheses have been put forward in an attempt to answer fundamental questions about the structure and history of the formation of aeolian cover deposits in northeastern Siberia (Kolpakov, 1983; Alekseev et al., 1984; Kut et al., 2015; Galanin, 2021). For example, sedimentary covers on the terraces of large rivers (Lena, Vilyui, Linde etc.) have been diversely attributed to alluvial-lacustrine genesis in the river valleys, “deluvial-proluvial and solifluction” deposits on the gentle slopes of interfluves, and eluvial

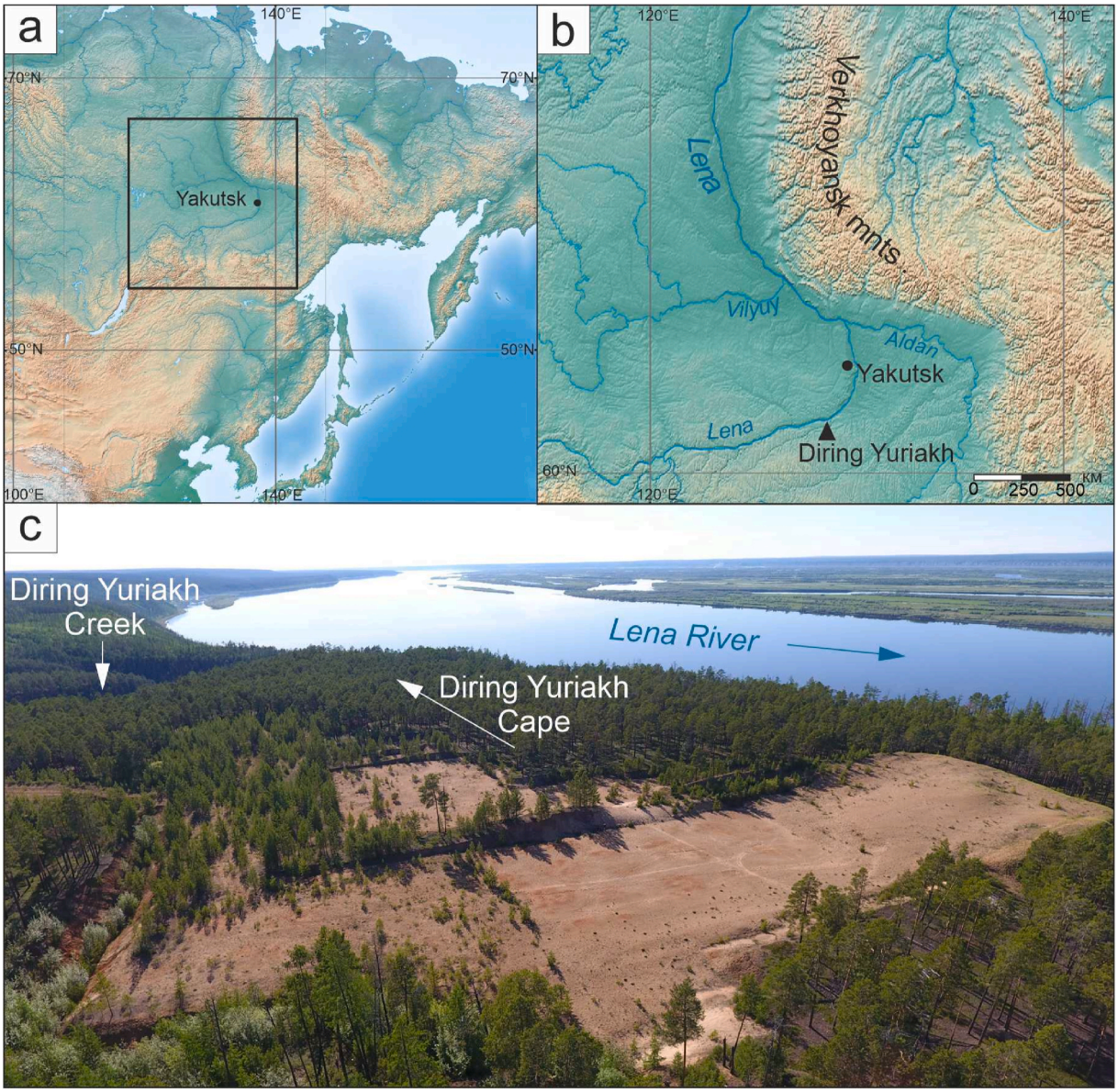

Fig. 1. a,b) The location of the Diring Yuriakh site; c) Photo of the Diring Yuriakh site from the top, looking towards the southwest.

processes in the watersheds (see reviews in Galanin and Pavlova, 2018; 2019). More recent studies have suggested that throughout the Quaternary, and across all of the Siberian plains including Central Yakutia, large-scale desertification processes played a significant role in both aeolian and non-aeolian sedimentation and landform development (Velichko et al., 2011). During various stages of the Middle and Late Quaternary, the relative importance of aeolian and fluvial processes – the two dominating landscape-building forces in the region – radically changed, and the formation of deflationary and accumulative aeolian relief intensified. The nature of these aeolian covers is deeply connected to dynamic changes in both climate and sedimentary process: for example, permafrost aggradation, syn- and epigenetic freezing, periodic advances of mountain glaciers, fluctuations in the level of watercourses and downcutting of the base level (Galanin and Pavlova, 2018; Galanin and Pavlova, 2019).

Aeolian deposits cover at least half of the territory in Central Yakutia and are characteristic of many cold regions of the world (Black, 1951; Wolfe et al., 2011; Seppälä, 2012). Aeolian sediments in the area are found in complex spatio-temporal relationships with other genetic types of Quaternary deposits (glacial, lacustrine, alluvial, cryogenic, etc.); this testifies to an alternation of cold hyper-arid and cool semi-arid wet epochs throughout the Quaterary (Galanin et al., 2016; Galanin and Pavlova, 2018). The dune massifs of Central Yakutia and Eastern Siberia are located in a continuous permafrost zone and represent thermal and geocryological anomalies of unknown origin. Ancient and modern dune deposits make up extended sections of river terraces and interfluves in Yakutia and eastern Siberia; they often overlie ancient glacial moraines, lacustrine, alluvial, and swamp deposits. For example, in various sections, one can find intact branches and trunks of forest vegetation of Bølling-Allerød age (Late Glacial interstadial; 14.5–12.9 ka), buried under Younger Dryas (late glacial stadial; 12.9–11.7 ka) dunes (Galanin, 2021). In any case, Late Pleistocene sand cover forms a significant part of the Lena River high terraces in Central Yakutia, but in this region, as in most of northeastern Siberia, there are very few detailed geochronological studies, and so the past environmental record preserved in these deposits is yet to be interpreted quantitatively. Based on remote mapping of dune formations using satellite images and GIS, about 1440 aeolian forms with a total area of 65,001 km^2 have been identified (Kut et al., 2015). The sand massifs are confined to four main areas located in the Lena, Khoruongka, Linde, Vilyui and Tyung rivers basins. Most forms of aeolian relief are distributed within the interfluve surfaces at levels of 160–190 m, less often at lower hypsometric levels in the Vilyui and Tyung valleys (90–120 m).

Central Yakutia is also famous for the Diring Yuriakh Early Paleolithic site located in the Lena River valley (Waters et al., 1997; Mochanov, 1993). The Diring Early Palaeolithic culture potentially represents one of the oldest traces of early humans at high latitudes (north of 60°N). Late Palaeolithic stone-tool assemblages have also been found at the site and these represent the Duktai culture of the Yakutia and Chukotka areas of northeastern Siberia. The Duktai is the first Late Paleolithic culture discovered in this part of the continent and it is believed to have existed in the second half of the Late Paleolithic (most likely 25-11 kyr, but possibly starting as early as 35 kyr). This culture is of great significance as its carriers are believed to be associated with the initial settlement of the Americas at the end of the Late Pleistocene (Mochanov, 1977). Unfortunately, the absence of absolute chronological control (Kirianov et al., 2024) has limited meaningful discussion of the implications of the site, making it difficult to test specific hypotheses regarding human dispersal to Beringia and the Americas.

In summary, the absence of chronological constraints on environmental archives in this complex and dynamic region leads to significant gaps in our understanding of past high-latitude climate change and Palaeolithic human dispersal. As such, to address the timing of Late Quaternary evolution of aeolian sedimentation and relief in the region, and to provide a new chronological framework for the regional Upper Palaeolithic archeology, we applied OSL dating to the Diring Yuriakh location for the first time. Specifically, we focus on a 120 m terrace containing a series of aeolian covers of various ages overlying a deflated surface containing numerous Early and Late Palaeolithic artefacts. This site has been known for some time, but the origins and age of these aeolian deposits remain a matter of speculation. Our work focuses on constraining the timing of the various aeolian sedimentation and deflation stages that occurred during the Late Pleistocene, and to provide a minimum age for the underlying Late Palaeolithic artefacts (the Duktai culture).

2. Study area

Diring Yuriakh is located on the oldest Tabagan terrace (VIII) of the Lena River in Central Yakutia (Fig. 1). The Diring Yuriakh site first received wide attention in 1982 when a few Neolithic burials were discovered. Further archaeological surveys by Mochanov and Fedoseeva (2007; 2013a) found two other archaeological complexes from the Late Palaeolithic and the Early Palaeolithic. Detailed archaeological and geological studies were carried out in 1983–1990, with the opening of 6 excavation areas, 11 trenches and 50 pits covering a total area of 36250 m^2 (Mochanov and Fedoseeva, 2007; 2013a). Archaeological material was found in four excavation areas, as well as in several trenches and pits located closer to a cape at the southwestern end of the terrace. At that time the main focus was on excavating the oldest known complex – the artefacts associated with the Diring Early Palaeolithic culture (Mochanov and Fedoseeva, 2013a; Waters et al., 1997). However, among the finds of the Early Palaeolithic stone tools at the cape of Diring Yuriakh, were artefacts that looked much younger. These included an end core; longitudinal scraper on a large flake, with a carefully decorated multi-row retouched working edge; a retouched pointed blade chip, a massive retouched point on a segment-shape; and other artefacts indicating a developed lithic technology (Kirianov et al., 2024). This complex also had a very different lithology (chert) compared to the older quartzite artefacts and only occurred in the part of the site located in the southwestern end of the terrace. Based on the technical and typological characteristics of this complex, it was assumed to be from the Late Palaeolithic (Mochanov, 1977). From a comparison of this “young” complex of Diring Yuriakh with the well-known Upper Paleolithic industries of the region (Yanskaya site, Chirkuo, Mungkharyma, Duktai culture locations), it was concluded that the Diring Yuriakh material should be considered part of the Duktai culture of norteastern Siberia (Pitulko et al., 2012; Mochanov and Fedoseeva, 2013a; Mochanov and Fedoseeva, 2013b; Kirianov et al., 2024). The Duktai technocomplex is characterized by a developed technique of prismatic splitting and, in the absence of absolute dating, the age of the culture remains debatable. However, it is generally believed that this industry existed in the northeastern part of Siberia during the Late Pleistocene - Early Holocene, at approximately 25-10 ka (Abramova, 1979), or perhaps from 35 ka according to some estimates (Mochanov, 1977).

Previous studies provide a firm stratigraphic basis for understanding Quaternary sediment deposition at Diring Yuriakh. The terrace deposits are subdivided into 16 stratigraphic layers (complete description according to Mochanov, 1992, 1993) or more generally 4 units (short description, according to Waters et al., 1999). Deposits are numbered from bottom to top. At the section base lies a foundation of Cambrian limestones, with the upper boundary 105 ± 2 m above the Lena River (layer 1). On top of the limestone lies a 0.5–1.2 m layer of basal pebbles (alluvium channel facies) (layer 2). The pebbles are overlain by layer 3 – coarse- and medium-grained sands, dark red, highly ferruginous. The sands are represented by a series of horizontally and cross-bedded sublayers (0.5–15.0 m). The top of layer 3 is affected by localized cryogenesis around large complex sand wedges. The sandy infilling of the ice wedges is distinguished as layer 4; the upper parts of the wedges are eroded. Above that, there is a gravel-pebble-boulder layer, identified as layer 5, which is characterized by scattered clusters of rock fragments representing a deflation surface. Almost all of this fragmentary material

has traces of wind erosion and desert patina/varnish (ventifacts) Layer 5 is covered by a series of layers consisting of aeolian sands and sandy loams (layers 6–10, with a total thickness up to 8–10 m). In the eastern part of the site, another series of sand layers up to 20 m thick (layers 11–13) are found. The top part of the section is covered by sands of different texture and structure (layers 14–16), yellowish-gray, horizontally layered with weakly developed palaeosols, permafrost veins and pseudomorphs, and with total thickness of ~5.0 m (Fig. 2).

The cultural layer, which includes the Duktai artefacts at Diring Yuriakh, is found on the deflation surface represented by layer 5 (Fig. 2), and is covered by different units of aeolian sands towards the cape of the terrace (Fig. 1). Deposits of layers 6–13 are absent on the Diring Yuriakh cape itself (Fig. 2), where layers 14–16 form the aeolian cover. These latter layers record patterns of aeolian sedimentation and are the main focus of this paper. In addition, the age of this aeolian cover at Diring Yuriakh would provide minimum age constraints on the Duktai Late

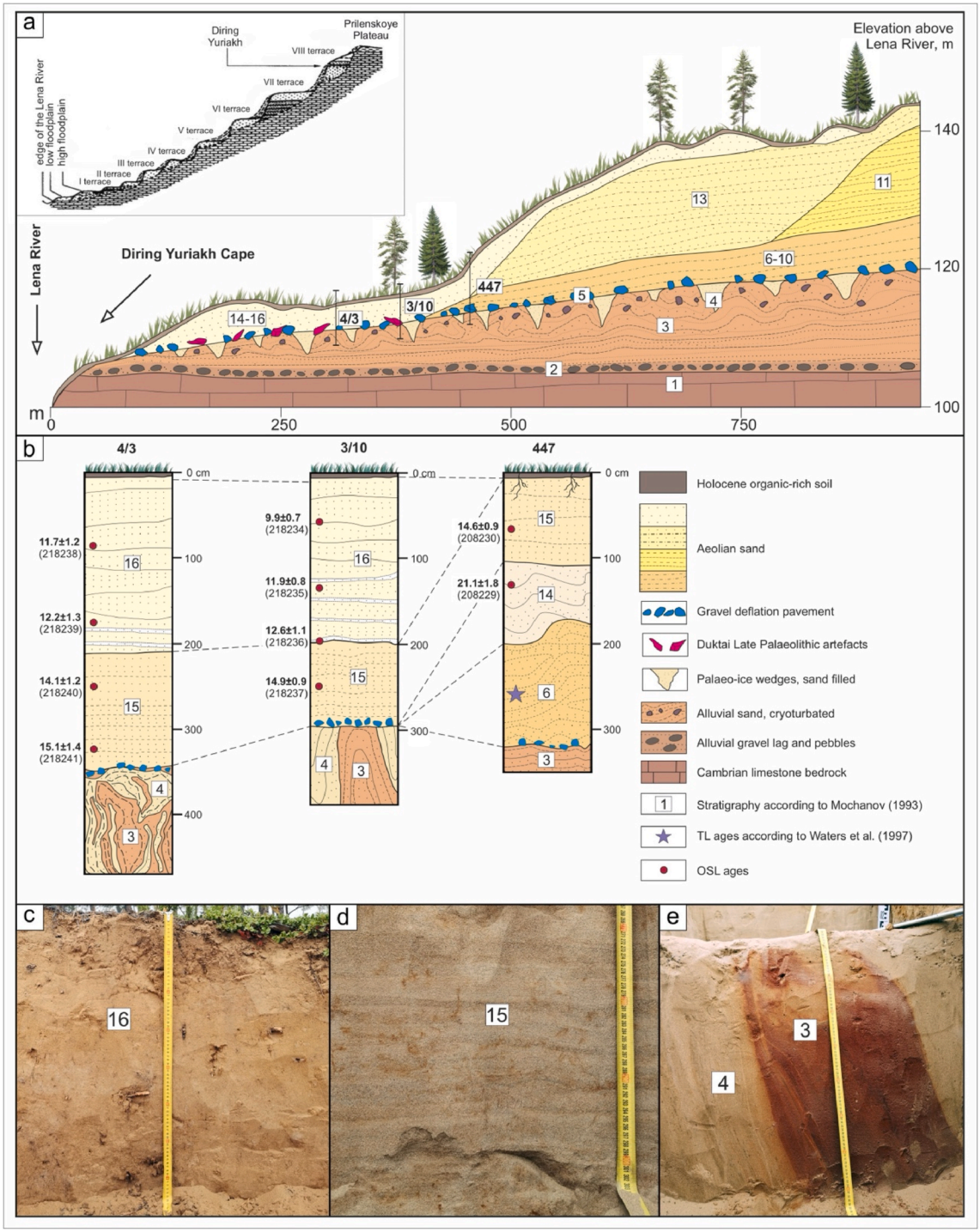

Fig. 2. a) Geomorphological and sedimentary layer profile of the Diring Yuriakh site with location of studied sections shown in black vertical lines and inset of the whole profile of the river terraces with the location of the Diring Yuriakh (according to Mochanov, 2007); b) Stratigraphic charts of the sampled sections; c,d,e) Photo of the aeolian sediments: c – layer 16, sands, section 3/10; d – layer 15, horizontal sand bedding, section 4/3; e – layer 3, reddish microdiapir in layer 4, section 3/10. Cryoturbation of layer 3 is localized around the ice wedges (layer 4). A thermoluminescence age of >260 ka has been obtained for layer 6 by Waters et al. (1997a), but this age remains controversial (Huntley and Richards, 1997; Kuznetsova et al., 2022).

Palaeolithic culture, as the Duktai artefacts underlie layer 15 at the cape (Fig. 2a), and allow reconstruction of the history of aeolian sedimentation along a central part of the Lena River.

3. Sampling and luminescence measurement protocols

A series of sections were excavated at Diring Yuriakh (Fig. 2); aeolian sediments were described and sampled for luminescence dating. The sections were chosen to capture as much as possble of the aeolian sedimentation at the end of the Pleistocene and so allow an understanding of the stratigraphic and chronological context of the Duktai Late Palaeolithic culture. The sandy sediments were sampled using tubes hammered horizontally into a cleaned section face. Sample preparation took place under subdued orange LED light – the outer parts at the ends of the tube were reserved for measurement of radioactivity, and the inner part for luminescence measurements. The inner part was processed using standard procedures (Murray et al., 2021): wet sieving to obtain the 180–250 μm sand fraction, treatment with 10% HCl, H_2O_2, HF, and repeated HCl. Separation of K feldspar and quartz was achieved via density separation (2.58 g cm^{-3}), using aqueous heavy liquid solution (LST, FastFloat™). Finally, the heavier quartz fraction was treated again with 40% HF to remove any remaining feldspar and the outer alpha-irradiated surface; this was followed by a final rinse with 10% HCl.

Cleaned quartz and K-rich feldspar grains from 12 samples were measured at the Nordic Laboratory for Luminescence Dating, Denmark. All measurements were made on multi-grain aliquots mounted on stainless steel cups (quartz ~8 mm diameter; feldspar ~2 mm diameter) and measured on a Risø TL/OSL model DA-20 reader equipped with a calibrated beta source (Hansen et al., 2018; Autzen et al., 2022). OSL was stimulated with blue light (470 ± 20 nm) and IRSL with infrared light (870 ± 40 nm). The quartz OSL signal was recorded using a U-340 filter and infrared stimulated luminescence from K-rich feldspar (IRSL), using a combination of blue filters (Thomsen et al., 2008).

Quartz dose estimates were made using a standard SAR protocol with preheating at 260 °C for 10 s, a cut heat at 220 °C, and blue-light stimulation at elevated temperature (280 °C) at the end of each SAR cycle (Murray and Wintle, 2000, 2003). The quartz OSL signal was measured for 40 s using blue stimulation at 125 °C; early background subtraction (first 0.32 s minus subsequent 0.32 s) was used to calculate the net signal. K-feldspar doses were estimated using the post-IR IRSL SAR protocol (Buylaert et al., 2012) with preheating at 320 °C for 60 s and IR stimulation at 50 °C (for 200 s) followed by IR stimulation at 290 °C (200 s) ($pIRIR_{50,290}$). Late background subtraction was used to calculate the net $pIRIR_{50,290}$ signal using the photon sum collected in the initial 2 s of stimulation, minus a sum based on the last 50 s. No correction was made for IRSL signal instability (Buylaert et al., 2012).

3.1. Dosimetry

Radionuclide concentrations were measured using high-resolution gamma spectrometry, calibration is described in Murray et al. (1987, 2018). The samples were dried at 110 °C, ground, ignited at 450 °C for 24 h, and mixed with molten high viscosity wax before casting in an aluminium mold; the resulting cup-shaped samples were stored for >20 days before counting. The derived ^{238}U, ^{226}Ra, ^{232}Th and ^{4}K activity concentrations were converted to dry infinite matrix dose rates according to Guérin et al. (2012). Corrections for water content based on Aitken (1985), and cosmic ray contributions on Prescott and Hutton (1994).

4. Results

4.1. Aeolian cover structure

During field studies, the cover sediments at Diring Yuriakh were studied at the southwestern end, where ancient layers of red sands (layer 3, here and below - according to Mochanov's stratigraphy) and the deflationary surface of ventifacts (layer 5) are covered by units of aeolian sand.

In this paper, we describe the structure of 3 sections that most fully characterize the history of aeolian sedimentation at Diring Yuriakh in the Late Pleistocene (Fig. 2). The positions of the sections are shown as 3 vertical black lines on the geomorphological profile in Fig. 2a. In the field, we described individual layers from each profile and correlated them with the stratigraphic scheme and layer numbering from Mochanov (1997).

Section **DY 4/3**.

- 0–210 cm: fine sands, massive structure, light brown, with whitish sand lenses and tube-like structures. In the lower 15 cm there are several bands (3–5 mm) of beige sand, possibly blown from the underlying sediments. Lower contact is clear;
- 210–340 cm: fine sands, light beige, lighter than Unit 1, with a grayish tint. The lower 250 cm are enriched with dark-colored minerals
- 340–345 cm: gravel up to 1 cm, the infilling contains red-colored sand of different grains;
- 345–460 cm: brownish-red and brown sands, sometimes massive and sometimes showing multidirectional layering due to cryoturbation.

Section DY 3/10.

- 0–200: sands, light brown, massive. From 120 cm depth, thin layers of fine whitish sand (2–3 mm) are observed, and from 135 cm - numerous lenses of this whitish sand. Vertical roots are developed along them, possibly of modern vegetation or Q_4;
- 200–290 cm: fine sands, well sorted, light yellow, grayish, with a clear alternation of dark (enriched by dark-colored minerals) and light bands 1–3 cm thick. At 290 cm, the intrusion of red-colored sands observed. At the base of the layer is an abundance of different-sized clastic material, including large pebbles 5–8 cm;
- 290–360 cm: red-colored highly ferruginous fine sands with vertical layering (microdiapir) embedded in light yellow sand with vertical layering.

Section 447.

- 0–110 cm: fine sands, light brown;
- 110–190 cm: fine sands, light brown, somewhere cryoturbated, lightly ferruginous and ochreous, with lenses of fine whitish sand;
- 190–310 cm: fine sands and sandy loams, slightly ocherous, with interlayers of humus horizons, cryoturbated in places.
- 310–340 cm: fine sands, brown, highly cryoturbated, at the top there are small and large ventifacts.

Based on lithological characteristics, the identified layers were cross-correlated with the known stratigraphy of Mochanov (see Fig. 2b). At the base of the sections, layers 3 and 4 are identified: likely Pliocene alluvial sediments that form the Tabagan terrace of the Lena (layer 3) with infilled sand wedges (layer 4). In section 447, furthest away from the modern Lena River, layer 3 is overlain by ancient aeolian deposits of layer 6 and sands and silts that represent Mochanov's layer 14. Layers 6 and 14 are only recorded in section 447, due to the higher elevation and better preservation. Aeolian sands of Mochanov's layer 15 were identified in all three sections, whereas layer 16 only is identified in sections DY 4/3 and DY 3/10. The top of each section is covered by a modern soil. At the cape, stone tools of the Late Paleolithic Duktai culture and Early Paleolithic Diring culture underlie layer 15, whereas only stone tools of the Diring culture haven been found under layer 6 further away from the Lena River (Fig. 2).

4.2. Luminescence chronology

4.2.1. Dose rate and water content

Radionuclide activity concentrations, and dry infinite matrix beta and gamma dose rates are presented in Table 1. Total water content in all samples is assumed to be 13 ± 4%. Dose rates calculated from gamma-spectrometry activity measurements rely on conversion factors (Guérin et al., 2012). The measured activity concentrations of ^{226}Ra, ^{232}Th and ^{40}K differ little from section to section, with overall ranges: ^{226}Ra – 11–18 Bq.kg^{-1}, ^{232}Th - 16–23 Bq.kg^{-1}, ^{40}K - 700–800 Bq.kg^{-1}. Although individual ^{238}U concentrations are insufficiently constrained to allow discussion of disequilibrium on a sample-by-sample basis, the average unweighted ^{226}Ra/^{238}U ratio (ignoring sample 218234 where the uncertainty on ^{238}U is >100%) is 1.00 ± 0.07 (n = 9). Thus, on average, we do not have any evidence for disequilibrium in the first part of the ^{238}U chain. Total dose rates are very similar across all sections, with an average of ~2.8 Gy.ka^{-1}.

4.2.2. Quartz OSL ages

Fig. 3a shows a representative natural OSL curve from a quartz aliquot of sample 208229 (D_e ~55 Gy), together with an OSL curve from calibration quartz (Hansen et al., 2018; Autzen et al., 2022); the latter is known to be dominated by the quartz OSL fast-component, and it is clear that this applies also to sample 208229. A typical dose response curve is given in Fig. 3b. The repeat point at 20 Gy lies on top of the first measurement showing that the SAR sensitivity correction is working well; the curve also passes through the origin indicating that recuperation is negligible. A dose recovery test was undertaken after bleaching aliquots twice at room temperature for 100 s under blue LEDs, separated by a 10 ks pause. The given dose was approximately equal to the natural dose, and the dose was then measured using our chosen protocol. This measurement was applied to aliquots from 8 samples and the average measured to given dose ratio is 0.97 ± 0.03 (n = 78). The quartz dose recovery results are shown in Fig. 3b. We conclude that our SAR protocol is able to measure, with sufficient accuracy, a known laboratory dose given before any thermal pretreatment.

5. Discussion

5.1. Reliability of luminesce ages

We evaluate the bleaching status of the samples at the time of deposition by examining the feldspar ages plotted against quartz OSL ages in Fig. 4b, and the corresponding ratios given in Table 2. Following Murray et al. (2012) and Møller and Murray (2015), we identify all quartz samples for which the IR_{50} age is less than or consistent with the OSL age as 'probably sufficiently bleached' (PSB in Table 2), and the samples for which the $pIRIR_{290}$ age is consistent with the quartz OSL ages as 'sufficiently bleached' (SB in Table 2). This identification is based on the differences in bleaching rates of these 3 signals. At the 95% confidence interval, all samples meet both criteria, and so we conclude that all quartz OSL signals were sufficiently bleached at deposition that any remaining signal was undetectable compared to the signal subsequently acquired during burial.

Table 1
Radionuclide concentrations and dry infinite matrix beta and gamma dose rates.

Lab. code	H, m	^{238}U, Bq/kg	^{226}Ra, Bq/kg	^{232}Th, Bq/kg	^{40}K, Bq/kg	Beta dose rate, Gy/ka	Gamma dose rate, Gy/ka
208229	130	8 ± 2	10.9 ± 0.3	16.6 ± 0.3	749 ± 9	2.12 ± 0.03	0.86 ± 0.01
208230	160	12 ± 2	12.0 ± 0.4	16.6 ± 0.3	688 ± 9	1.96 ± 0.02	0.82 ± 0.01
218234	50	5 ± 7	16.5 ± 0.6	24.0 ± 0.6	814 ± 14	2.38 ± 0.04	1.04 ± 0.02
218235	140	15 ± 8	16.0 ± 0.6	23.6 ± 0.6	814 ± 14	2.23 ± 0.04	1.03 ± 0.02
218236	200	14 ± 2	13.3 ± 0.3	19.6 ± 0.3	791 ± 8	2.26 ± 0.02	0.95 ± 0.01
218237	260	17 ± 3	18.3 ± 0.4	25.2 ± 0.3	795 ± 9	2.36 ± 0.03	1.05 ± 0.02
218238	90	15 ± 2	13.4 ± 0.3	20.6 ± 0.3	805 ± 9	2.31 ± 0.02	0.97 ± 0.01
218239	185	12 ± 5	12.6 ± 0.4	18.0 ± 0.4	804 ± 11	2.28 ± 0.03	0.93 ± 0.01
218240	260	15 ± 2	15.9 ± 0.3	23.0 ± 0.2	780 ± 6	2.28 ± 0.02	1.00 ± 0.01
218241	330	20 ± 5	11.6 ± 0.4	17.8 ± 0.5	784 ± 14	2.22 ± 0.04	0.91 ± 0.02

5.2. Aeolian sands of Central Yakutia – characteristics and previous work

Questions on the age and genesis of wavy- and cross-stratified quartz sands and loams of Central Yakutia have been discussed for more than half a century. A number of researchers consider these sediments to be dune covers that formed as a result of radical desertification during MIS 2–4 (Kolpakov, 1983; Alekseev et al., 1984; Galanin et al., 2016; Waters et al., 1999). However, these sand covers and sandy loams of Central Yakutia, located at a different hypsometric levels, but almost identical in composition, structure and facies characteristics, were for a long time attributed to different processes and considered as completely different genetic types due to the lack of detailed sedimentological descriptions and absolute ages (Galanin and Pavlova, 2019).

Analyses of the satellite images of Central Yakutia show that this territory is characterized by active development of aeolian relief forms (Kut et al., 2015). These modern-recent aeolian covers are a result of active reworking of underlying sands during changes in climate in the Middle/Upper Pleistocene and Holocene.

According to the geomorphological conditions, facies composition and fragmentary geochronological data, these formations are often correlated with the deposits of the Dolkuma Formation, a regionally developed thick unit of aeolian sands, characterized in the reference sections of Peschanaya Gora, Diring-Yuryakh and Ust-Botuoma in the middle reaches of the Lena River (Kolpakov, 1983; Alekseev et al., 1984; Kamaletdinov and Siegert, 1989; Waters et al., 1999). The aeolian origin of the Dolkuma formation is evidenced by the following features (Galanin and Pavlova, 2019): lithological (sandy loam composition, presence of ventifacts, fragments of soil horizons, high porosity); sedimentological (smooth layering, interbedding of cross-stratified and horizontally layered units), geomorphological (coverage, the presence of wavy surfaces of buried relief) and permafrost-hydrogeological (low ice content, absence of polygonal ice, etc.).

Some of the first studies on the aeolian origin of Late Pleistocene sandy deposits of Central Yakutia were undertaken by Kolpakov (1983). He emphasized that the aeolian formation in Yakutia is represented by three facies – deflationary surfaces of rocky deserts, sands and, aeolian dust covers. The facies of deflationary deserts represent spaces that were eroded as a result of wind activity that carried sand and dust. If the deflated sediments included rock fragments, boulders or pebbles, these were polished by sand, partly crushed and turned into ventifacts and faceted stones concentrated on the surface. Aeolian sand facies are often blown as mantles and ridges onto rocks and alluvial sediments. In Central Yakutia, aeolian sands are characterized by horizontal structure rather than cross-bedding. The aeolian dust facies (Yedoma) is widespread in Yakutia. The predominant part of the sediments is in complex with wedge ice of the syngenetic type (called cryogenic-aeolian); this concentrates around river terraces and in the lower reaches of the Lena River can be found at heights up to 230 m.

Currently, in Central Yakutia, the reference section for the Dolkuma formation is the Kysyl-Syr sand massif. At the base of the section lie alluvial deposits 10–12 m thick; the formation of these alluvial deposits is attributed to the end of MIS 4-2; ~65-28 ka (Galanin et al., 2016). Overlying dune deposits with a maximum thickness of up to 22–24 m are

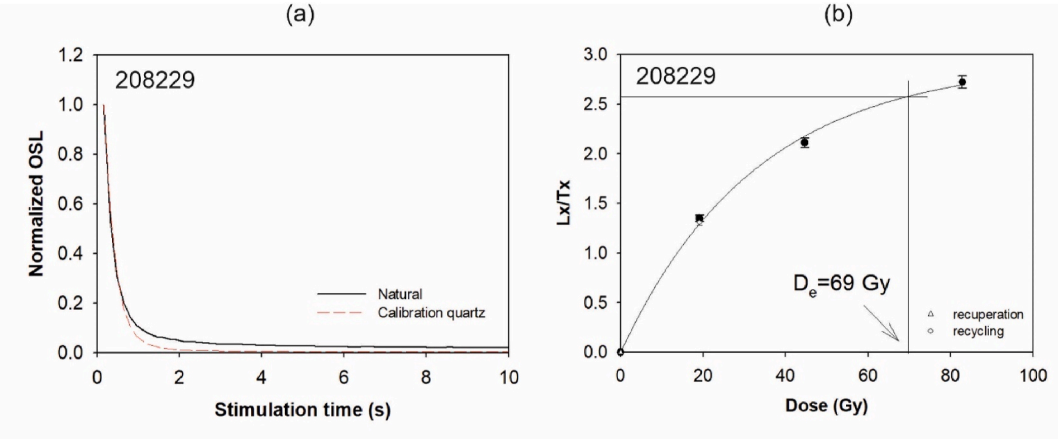

Fig. 3. (a) Natural OSL curve from sample 208229 compared to calibration quartz. (b) Representative dose response curve for sample 208229, showing recycling and recuperation data points, and fitted with a single saturating exponential model. The sensitivity corrected natural OSL signal is interpolated onto the fitted curve to give the D_e for this aliquot.

represented by packages of horizontally, wavy-laminated, rarely cross-laminated, medium and fine quartz sands, separated by deflationary surfaces with thin layers of coarse quartz sand and single fine gravel. Noticeable changes in climate and its gradual amelioration are evidenced by the upper aeolian units of microbanded sandy loams. These begin to contain single vertical roots and thin rudimentary soil layers, which alternate with well-sorted quartz sand. This indicates a decrease in the activity of aeolian processes towards the Holocene (Galanin et al., 2016).

Recent radiocarbon dating results and data on the structure of new reference sections (Kyzyl-Syr) clearly demonstrated that the cover sands with horizontal layering, comprising the upper parts of both the lowest and highest terraces in the middle reaches of the Lena River, are of the same age and were deposited simultaneously during MIS-2 (Galanin and Pavlova, 2019). However, radiocarbon dating of aeolian sands is difficult because of low organic contents and reworked organic material during sand transport events. As such, detailed luminescence dating is required to understand the nature of sand activity in the Late Pleistocene.

5.3. New luminescence-based age constraints on the Central Yakutia aeolian sands

Our luminescence dating results combined with lithostratigraphic interpretations show that the recent phase of aeolian sedimentation at the site developed in a complex series of stages, and its initiation roughly coincided with the LGM (MIS 2), reflecting the aridification of the climate in Yakutia.

The earliest age of 21.1 ± 1.8 ka from section 447 (layer 14) places an upper age constraint on the initiation of aeolian sedimentation, as well as the reworking processes that spread sand dune massifs and covers in the region, during the Late Pleistocene. A thermoluminescence (TL) age of >260 ka was presented by Waters et al. (1999) for layer 6, but this age has been challenged on methodological grounds relating to the shortcomings of the dating method (Huntley and Richards, 1997) and stratigraphic considerations (Kuznetsova et al., 2022). Nevertheless, the TL age indicates the presence of a substantial hiatus that presumably reflects extensive aeolian deflation and reworking of sediments before c. 21 ka. In general, the aeolian sediment units in the section are distinguished by their light color, as well as the presence of ochre horizons,; these characteristics indicate oxidizing conditions during accumulation – good aeration and high dryness. This aridification of the region led to the almost complete disappearance of tree vegetation in Central Yakutia, and the spread of cryosteppe and rocky semi-desert landscapes. Relatively big rivers often dried up completely, and in some wind-blown interfluve areas the soil and vegetation cover was completely denuded; active deflation led to the removal of fine particles and the formation of rocky deserts with ventifacts. It is hypothesized that large dune massifs arose on river terraces at this time, moving in a southeastern direction, and fed by deflation of dried and denuded floodplain material (Galanin et al., 2016). The peak MIS 2 (last glacial maximum; LGM) age from layer 14 in section 447 confirms that aeolian sand activity occurred at this time of peak aridity and low temperature. The absence of this layer in other sections (4/3 and 3/10), along with the apparent substantial time gap separating layer 14 from layer 6, suggests active processes of aeolian reworking, and as a result a large portion of material at the Diring Yuriakh location has been removed.

The second period of aeolian activation is represented by a group of ages between 15 and 14 ka from Mochanov's layer 15 (Fig. 2). This cluster is centered on the boundary between the end of Heinrich event 1/Older Dryas cold conditions and the onset of the Late Glacial interstadial (Bølling-Allerød) warming at c. 14.5 ka. One possible interpretation of these ages is that the spread of vegetation cover on sandy massifs did not immediately respond to climate warming, and so dune activity during the cold Late Pleniglacial conditions did not cease abruptly with the onset of the Late Glacial,. A clear hiatus between layers 15 and 14 is seen in the new chronology, which suggests that aeolian deflation dominated the period ~20-15 ka.

Our ages from layer 16 cluster between c. 12.6 and 9.9 ka, which corresponds well with the Late Glacial stadial/Younger Dryas cooling event (Fig. 2). We suggest that as a result of this climate cooling and aridification, alluvial sands in the valley bottom have become more prone to deflation. Following the Younger Dryas, at the beginning of the Holocene, there was a sharp warming, which was not accompanied by an equivalent rise of humidity, and annual precipitation remained below the modern level through the whole Early Holocene (Velichko et al., 1997; Andreev and Klimanov, 2005). Aeolian sedimentation did not cease instantly at the Late Glacial – Holocene transition. This process was rather gradual, because vegetation cannot immediately colonise sandy areas when the precipitation is limited. The youngest age of 9.9 ± 0.7 ka from the top of section 3/10 presumably reflects the cessation of aeolian sedimentation in the second half of the Early Holocene. After 10 ka, apparently, the entire slope of the Lena valley was already covered with dense vegetation (probably forest); this broke the connection between the terrace and the river channel – the source of the aeolian sand.

In summary, the source of the aeolian sand cover at Diring Yuriakh was the alluvium of the Lena River, with aeolian redeposition of sands from riverbed banks and low terraces of the Lena River. The areas of sand massifs exposed in the Lena River channel during the low-water season are large enough in any climatic period. However, for these

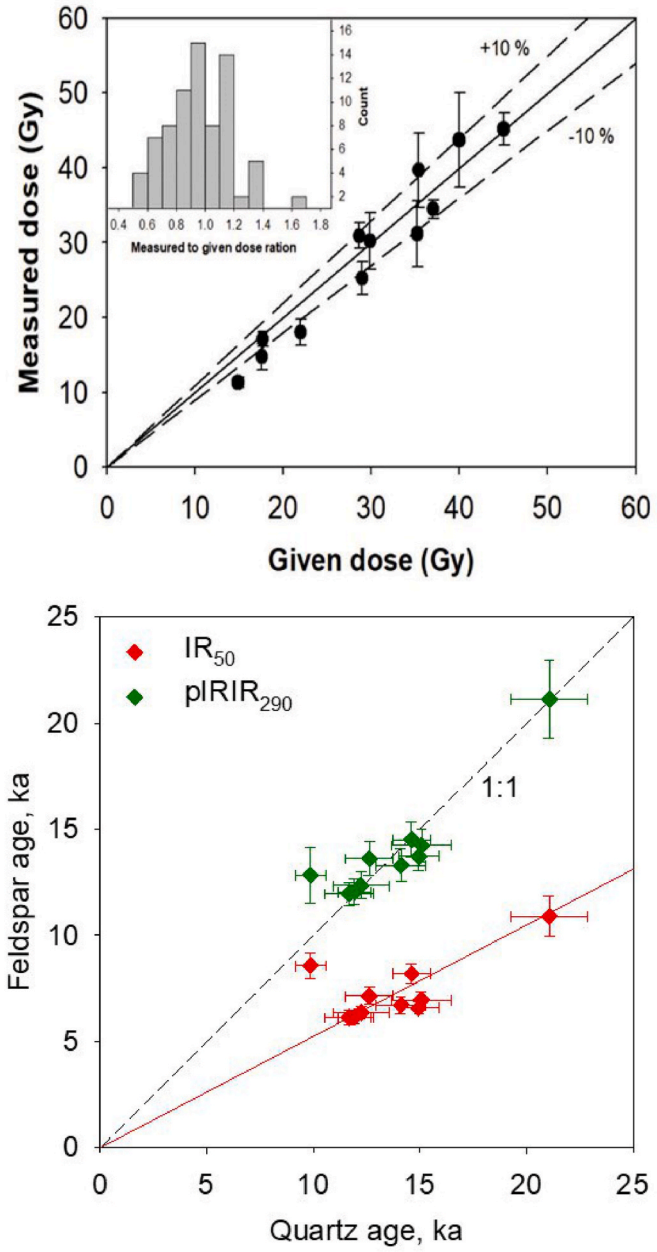

Fig. 4. (a) Results of the quartz dose recovery test: measured dose plotted as a function of the given dose for 8 samples (some samples have been given more than one dose in a dose recovery test); the same data but now for every aliquot individually is shown as a histogram inset. (b) Feldspar IR_{50} (red) and $pIRIR_{290}$ ages (green) plotted as a function of quartz ages.

sands to be blown up and transported to high terraces, they must dry quickly when the water level drops, and the valley slope must not be covered with vegetation that hinders the transport of sand from bottom to top. Periods of aeolian activity are therefore found to correlate well with changes in temperature and associated changes in humidity. In other climate zones and in smaller river valleys, the relation between aeolian activity and climate may be different. For example, in the valley of the Vychegda River in northeastern Europe, which is smaller than the Lena River and located in a area with less continental climate conditions, an increase in aeolian activity is noted between 17 and 10.5 ka (Zaretskaya et al., 2024). This is attributed to an increase in river flow after the LGM, which caused the formation of large sand massifs (alluvial bars) - sources of sand. There was no relation to the Late Glacial climatic epochs, because the main factor of aeolian activity in this case was the availability of sandy material and permafrost melting (Zaretskaya et al., 2024). However, aeolian activity ceased at c. 10.5 ka, similar to the Lena River valley, which was probably also caused by the delayed spread of vegetation after the onset of the Holocene.

Our results correlate well with existing interpretations of the Late Pleistocene aeolian deposits of the Dolkuma Formation (Kamaletdinov and Minyuk, 1991; Pravkin et al., 2018), and provide a more nuanced insight into the millennial-scale dynamics of aeolian activity at the end of the Late Pleistocene; one in which stadial-interstadial dynamics controls aeolian deposition and deflation. Indeed, the dune sands of Diring Yuriakh can be safely attributed to the Dolkuma Formation, and similar sediments are described in the Kysyl-Syr (Galanin et al., 2016; Galanin, 2021), Peschannaya Gora (Alekseev et al., 1984), and Ust-Boutom sections (Vasilieva et al., 2024).

Based on our ages and stratigraphic interpretation, we propose that several general phases of aeolian accumulation and deflation are recorded at Diring Yuriakh.

(1) The first phase is recorded in layer 5 – a deflation surface with well-defined ventifacts and archaeological artefacts of both the Early Palaeolithic Diring culture and the Late Palaeolithic Duktai culture, with the latter only found at the cape (magenta artefacts in Fig. 2a). The age of the deflation event exceeds the age limit of luminescence dating, but published TL ages suggest that the overlying layer 6 is older than 260 ka (Waters et al., 1997). If this TL age is correct (it has been questioned by e.g. Kuznetsova et al., 2022), the ventifacts imply that deflation was a dominant process here over extended time periods. This resulted in all the Quaternary deposits pre-dating layer 6 being eroded from the terrace surface, exposing Pliocene red sands and pebbles. Another possible interpretation is that there were repeated phases of deposition and erosion with no net accumulation, and potentially some erosion of the Pliocene alluvia. But even in this scenario, there must have been extended periods of deflation to create the ventifacts.

(2) The second phase is connected with the accumulation of layer 6, an aeolian sand unit that increases in thickness towards the interfluve. The TL age of Waters et al. (1997) suggests that this layer accumulated before the Late Pleistocene. More accurate dating would likely show a significant hiatus between phases 1 and 2, and constrain the age of the Early Palaeolithic artefacts of the Diring culture, which are found in some parts of the site below layer 6.

(3) After the accumulation of layer 6, a long period of net deflation can be inferred, which may have included alternating phases of deflation and accumulation. This process probably eroded parts of layer 6 and any other sediments above. Based on our results and existing data, this erosional phase in the region started before the Late Pleistocene and lasted until ~21 ka.

(4) A relatively poorly constrained phase of aeolian accumulation around 21.1 ka is recorded in layer 14, coinciding with the late LGM, when sand accumulation was accompanied by short periods of relief stabilization (ephemeric palaeosols) and cryogenesis (pseudomorphs).

(5) Reworking of these sediments occurred towards the end of MIS 2, when the top part of layer 14 was eroded and a hiatus from ~20 to ~15 ka is recorded. The sediments at the terrace close to the Lena River valley were completely eroded, presumably due to intense dune movement and aeolian activity/deflation at the time.

(6) A new phase of accumulation from 15.1 to 14.1 ka resulted in the formation of layer 15. Aeolian activity and dune formation at this point are associated with the cold conditions of the Older Dryas.

(7) Climatic amelioration at the onset of the Late Glacial interstadial/Bølling-Allerød led to preservation of the set of aeolian dunes that

Table 2
Summarises the D_e estimates, together with the number of accepted and rejected aliquots for each sample and signal. Aliquots were rejected if they fell outside1.5 times the interquartile range (Tukey, 1977). The total dose rates to quartz are then given; those to feldspar can be derived by adding 0.94 Gy.ka^{-1}, followed by the ages based on the three luminescence signals. The final columns give the IR_{50} to OSL and $pIRIR_{290}$ age to OSL age ratios.

Lab. code	H, m	Equivalent dose (Gy) and number of aliquots (n_r – rejected, n_a – accepted)						Total quartz dose rate, Gy/ka	Age, ka			Feldspar/Quartz Age Ratios		PSB	SB
		OSL		$pIRIR_{290}$		IR_{50}									
		D_e, Gy	n_r/n_a	D_e, Gy	n_r/n_a	D_e, Gy	n_r/n_a		OSL	$pIRIR_{290}$	IR_{50}	IR_{50}/OSL	$pIRIR_{290}$/OSL		
208229	130	54.8 ± 3.6	0/20	74.9 ± 5.6	0/9	38.7 ± 3.0	1/5	2.60 ± 0.13	21.1 ± 1.8	21.1 ± 1.8	10.9 ± 1.0	0.52 ± 0.06	1.00 ± 0.12	✓	✓
208230	160	35.6 ± 1.0	2/16	49.0 ± 1.8	0/6	27.7 ± 1.2	0/6	2.44 ± 0.12	14.6 ± 0.9	14.5 ± 0.8	8.2 ± 0.5	0.56 ± 0.05	0.99 ± 0.08	✓	✓
218234	50	29.8 ± 1.4	1/32	50.8 ± 4.6	0/8	34.0 ± 2.0	0/8	3.02 ± 0.15	9.9 ± 0.7	12.8 ± 1.3	8.6 ± 0.6	0.87 ± 0.09	1.30 ± 0.16	✓	✓
218235	140	35.3 ± 1.2	1/33	47.0 ± 1.0	0/8	24.0 ± 0.7	0/8	2.96 ± 0.15	11.9 ± 0.8	12.0 ± 0.6	6.2 ± 0.3	0.52 ± 0.04	1.01 ± 0.08	✓	✓
218236	200	35.1 ± 2.5	0/21	50.8 ± 1.9	0/8	26.6 ± 1.0	0/8	2.78 ± 0.14	12.6 ± 1.1	13.6 ± 0.8	7.1 ± 0.4	0.57 ± 0.06	1.08 ± 0.11	✓	✓
218237	260	43.9 ± 1.3	2/21	53.2 ± 1.1	0/6	25.5 ± 0.6	1/7	2.94 ± 0.15	14.9 ± 0.9	13.7 ± 0.7	6.6 ± 0.3	0.44 ± 0.03	0.92 ± 0.07	✓	✓
218238	90	33.3 ± 2.8	0/24	45.4 ± 0.5	0/8	23.2 ± 0.9	0/8	2.85 ± 0.14	11.7 ± 1.2	12.0 ± 0.6	6.1 ± 0.3	0.52 ± 0.06	1.02 ± 0.11	✓	✓
218239	185	34.0 ± 3.1	2/18	45.9 ± 1.1	1/7	23.7 ± 0.4	1/7	2.78 ± 0.14	12.2 ± 1.3	12.3 ± 0.6	6.4 ± 0.3	0.52 ± 0.06	1.01 ± 0.12	✓	✓
218240	260	40.0 ± 2.5	0/23	50.2 ± 1.9	0/8	25.4 ± 1.2	0/8	2.83 ± 0.14	14.1 ± 1.2	13.3 ± 0.8	6.7 ± 0.4	0.48 ± 0.05	0.94 ± 0.10	✓	✓
218241	330	40.6 ± 3.1	0/20	51.9 ± 1.5	0/8	25.3 ± 1.0	0/8	2.70 ± 0.14	15.1 ± 1.4	14.2 ± 0.8	7.0 ± 0.4	0.46 ± 0.05	0.95 ± 0.10	✓	✓

Note: 1. H – height; PSB – probably sufficiently bleached; SB – sufficiently bleached.
[2]Aliquots were rejected if they did not lie within 1.5 times the interquartile range (Tukey, 1977).
[3]feldspar dose rates can be derived from quartz dose rates by adding 0.94 Gy/ka.

stabilized at this time (layer 15, increasing in thickness toward the Lena River valley). The presence of ephemeric palaeosols suggests a milder climate and more developed vegetation in the region. Since this layer is the oldest cover of the Late Palaeolithic artefacts of the Duktai culture, our new chronological data provides a minimum age of these assemblages of >15 ka.

(8) A new phase of aeolian accumulation began around 12.6 ka and lasted until 9.9 ka. The onset broadly coincides with the Late Glacial stadial (Younger Dryas), when climate cooling and drying likely led to decreased vegetation cover and therefore enhanced sediment availability.

(9) After 10 ka, the warmer and milder climate of the Holocene resulted in widespread forest vegetation, which fixed and stabilized the sand cover.

5.4. Correlation with regional and global palaeoclimate

The new results underscore the existence of arid climate conditions in Central Yakutia during MIS 2. Pollen data from Lake Billyakh indicate that the glacial climate was significantly colder and drier than present (Tarasov et al., 2013; Diekmann et al., 2017). Similar evidence of aridity is found in records from Lake Elgygytgyn in Chukotka (Melles et al., 2007). Furthermore, studies of the ice-cover history in the Verkhoyansk Mountains (Stauch and Gualtieri, 2008; Stauch and Lehmkuhl, 2010) and the Chersky Range (Nørgaard et al., 2023) also suggest that the ice cover during MIS 2 was significantly reduced compared to MIS 6, most likely because the moisture input to Yakutia was minimal during MIS 2 (Stauch and Gualtieri, 2008; Stauch and Lehmkuhl, 2010). Nevertheless, the climate history of eastern Siberia aligns with large-scale trends in the Northern Hemisphere in the sense that aeolian sediments were deposited during globally colder periods. This trend is observed in paleoenvironmental signals along the eastern Siberian coastline, where silt- and ice-rich Yedoma formation sediments indicate more arid conditions and colder summer and winter temperatures during MIS 2 (Meyer et al., 2002; Wetterich et al., 2014; Schirrmeister et al., 2017). Yedoma formation in the Late Pleistocene likely resulted from aquatic and aeolian processes during extremely cold glacial climates and periglacial landscape conditions (Strauss et al., 2017), emphasizing the severe aridity of the Last Glacial Maximum that is also evidenced by the timing of deposition of aeolian sand at Diring Yuriakh.

6. Conclusion

We provide the first detailed study of the chronology of the sequence of aeolian covers at Diring Yuriakh in Central Yakutia. Quartz OSL and feldspar $pIRIR_{290}$ ages are in good agreement, allowing us to conclude that the quartz grains were sufficiently bleached before deposition. Our sections at Diring Yuriakh allow the identification of 6 sedimentary units, reflecting the main stages of aeolian accumulation in Central Yakutia during the end of the Late Pleistocene. Based on the new OSL chronology and existing TL data, 9 broad stages of aeolian activity have been identified: (1) Mid-Pleistocene (probably >260 ka) – the beginning of cryoaridization is recorded by a deflationary surface with ventifacts and early Palaeolithic artefacts; (2) Mid-Pleistocene (probably >260 ka) – a period of active accumulation with burial of the deflationary surface under aeolian sands (layer 6). (3) >21 ka – a long period dominated by deflation during which layer 6 eroded away close to the cape where the Duktai stone tools are found. (4) Around 21 ka – a phase of aeolian accumulation that coincided with the LGM; this is recorded in layer 14 with brief periods of incipient palaeosol formation and cryogenesis. (5) 20-15 ka – reworking of layer 14 which resulted in a hiatus due to localized aeolian activity and deflation. Layer 14 eroded away completely close to the cape, but the lower part of layer 14 remains intact further away from the river. (6) 15-14 ka – a period of accumulation (layer 15) that coincides with the Older Dryas. (7) ~14-13 ka – stabilization of the aeolian dunes during the late glacial interstadial/Bølling-Allerød. The stabilization of the dunes was associated with ephemeric palaeosol formation and more developed vegetation. Layer 15 is the oldest cover of the Late Palaeolithic artefacts of the Duktai culture, thus providing a minimum age of these assemblages of ~15 ka.

(8) ~12.5-10 ka – a new phase of aeolian accumulation (layer 16) that coincided with the Younger Dryas cold period and the very beginning of the Holocene. (9) <10 ka – dune stabilization and increased vegetation during the Holocene interglacial. The new OSL chronology indicates that the uppermost aeolian sands at Diring Yuriakh (layers 14–16) are well correlated with the sandy deposits of the Dolkuma Formation, which are recorded in many sections of Central Yakutia.

CRediT authorship contribution statement

Mariya S. Lukyanycheva: Visualization, Writing – original draft, Writing – review & editing. **Roger N. Kurbanov:** Conceptualization, Data curation, Investigation, Project administration, Supervision, Writing – original draft, Writing – review & editing. **Natalia A. Taratunina:** Formal analysis, Methodology. **Anzhela N. Vasilieva:** Investigation. **Vasiliy M. Lytkin:** Investigation. **Andrei V. Panin:** Investigation, Supervision, Writing – review & editing. **Anton A. Anoikin:** Investigation, Writing – original draft, Writing – review & editing. **Thomas Stevens:** Conceptualization, Supervision, Writing – review & editing. **Andrew S. Murray:** Methodology, Writing – review & editing. **Jan-Pieter Buylaert:** Formal analysis, Methodology, Writing – review & editing, Funding acquisition. **Mads F. Knudsen:** Conceptualization, Data curation, Investigation, Supervision, Writing – original draft, Writing – review & editing.

Declaration of competing interest

The authors declare that they have no known competing financial interests or personal relationships that could have appeared to influence the work reported in this paper.

Data availability

Data will be made available on request.

Acknowledgements

This study was supported by project N№ 21-17-00054 “Quaternary aeolian relief and cover deposits of Lena River basin (Eastern Siberia): structure, age and paleoenvironment significance” (field geological studies) and was partly supported by nordforsk.org through funding to “The timing and ecology of the human occupation of Central Asia” project number 105204 (luminescence dating). ML, RK, AV, VL, AP, and AA could not indicate any Russian affiliations due to restrictions imposed by Danish universities on joint publications of their staff with employees of the Russian state.

References

Abramova, Z.A., 1979. On the question of the age of the Aldan Palaeolithic. Sovetskaya Archeologiya 4, 5–14 (in Russ.).

Aitken, M.J., 1985. Thermoluminescence Dating. Academic Press, London.

Alekseev, M.N., Kamaletdinov, V.A., Grinenko, O.V., 1984. Cenozoic deposits of the Lena and Aldan. In: 27th International Geological Congress. Yakut ASSR, Siberian Platform. Generalized Guide of Excursions 052, 053, 054, 055. Nauka, Novosibirsk, pp. 21–42 (in Russ. and in Eng.).

Andreev, A.A., Klimanov, V.A., 2005. Lateglacial and Holocene in east Siberia (based on data obtained mainly in Central Yakutia). In: Velichko, A.A., Nechaev, V.P. (Eds.), Cenozoic Climatic and Environmental Changes in Russia, vol 382. Geol. Soc. Am. Spec. Pap., pp. 98–102. https://doi.org/10.1130/0-8137-2382-5.89

Arzhannikov, S.G., Arzhannikova, A.V., Chebotarev, A.A., Torgovkin, N.V., Semikolennykh, D.V., Lukyanycheva, M.S., Kurbanov, R.N., 2024. Experience of applying the cosmogenic dating method (^{10}Be) to assess the age and scale of the Pleistocene glacation in Northeastern Siberia (based on the example of glacier complexes of the Chersky ridge). Geomorfologiya I Paleogeografiya (in press), in Russ.).

Autzen, M., Andersen, C.E., Bailey, M., Murray, A.S., 2022. Calibration quartz: an update on dose calculations for luminescence dating. Radiat. Meas. 157, 106828 https://doi.org/10.1016/j.radmeas.2022.106828.

Barr, I.D., Clark, C.D., 2012. Late Quaternary glaciations in Far NE Russia; combining moraines, topography and chronology to assess regional and global glaciation synchrony. Quat. Sci. Rev. 53, 72–87. https://doi.org/10.1016/j.quascirev.2012.08.004.

Black, R.F., 1951. Eolian deposits of Alaska. Arctic 4 (2), 89–111.

Buylaert, J.-P., Jain, M., Murray, A.S., Thomsen, K.J., Thiel, C., Sohbati, R., 2012. A robust feldspar luminescence dating method for Middle and Late Pleistocene sediments. Boreas 41, 435–451. https://doi.org/10.1111/j.1502-3885.2012.00248.x.

Diekmann, B., Pestryakova, L., Nazarova, L., Subetto, D., Tarasov, P.E., Stauch, G., Müller, S., 2017. Late Quaternary lake dynamics in the Verkhoyansk Mountains of Eastern Siberia: implications for climate and glaciation history. Polarforschung 86 (2), 97–110. https://doi.org/10.2312/polarforschung.86.2.97.

Galanin, A.A., 2021. Late Quaternary sand covers of Central Yakutia (Eastern Siberia): structure, facies composition and paleoenvironment significance. Cryosphera Zemli 25 (1), 3–34.

Galanin, A.A., Pavlova, M.R., 2018. Late Quaternary dune formations (D'olkuminskaya series) in Central Yakutia (Part 1). Cryosphera Zemli XXII (6), 3–15 (in Russ.).

Galanin, A.A., Pavlova, M.R., 2019. Late Quaternary dune formations (D'olkuminskaya series) in central Yakutia (Part 2). Cryosphera Zemli XXIII (1), 3–15 (in Russ.).

Galanin, A.A., Pavlova, M.R., Shaposhnikov, G.I., Lytkin, V.M., 2016. Tukulans: sand deserts of Yakutia. Priroda (11), 44–55 (in Russ.).

Guérin, G., Mercier, N., Nathan, R., Adamiec, G., Lefrais, Y., 2012. On the use of the infinite matrix assumption and associated concepts: a critical review. Radiat. Meas. 47, 778–785. https://doi.org/10.1016/j.radmeas.2012.04.004.

Hansen, V., Murray, A., Thomsen, K., Jain, M., Autzen, M., Buylaert, J.-P., 2018. Towards the origins of overdispersion in beta source calibration. Radiat. Meas. 120, 157–162. https://doi.org/10.1016/j.radmeas.2018.05.014.

Kamaletdinov, V.A., Minyuk, P.S., 1991. The structure and characteristics of sediments of the Bestyakh terrace on the middle Lena River. Byulleten Comiss. po Izuchen. Chetvert. Per. 60, 68–78 (in Russ.).

Kamaletdinov, V.A., Siegert, K., 1989. Brief lithological characteristics of Cenozoic deposits of archeological site Diring-Yurakh (Middle Lena). In: Pleistocene Sibiri. Nauka, pp. 126–131 (in Russ.).

Kirianov, N.S., Anoikin, A.A., Vikulova, N.O., Kolobova, K.A., Bocharova, E.N., Chistyakov, P.V., Lukyanycheva, M.S., Kurbanov, R.N., 2024. Early Paleolithic complex of artifacts from the Diring-Yuryakh site (Central Yakutia): a new look. Stratum plus 1, 71–90. https://doi.org/10.55086/sp2417190 (in Russ.).

Kolpakov, V.V., 1983. Aeolian Quaternary deposits in the Lena area of Yakutia. Byulleten Comiss. po Izuchen. Chetvert. Per. 52, 123–131 (in Russ.).

Kut, A.A., Chzhan, T.R., Gurinova, S.A., 2015. Spatial analyze of dune (tukulan) distribution in Central Yakutia. Razvedka i Ohrana Nedr. 11, 13–17 (in Russ.).

Kuznetsova, T.V., Wetterich, S., Matthes, H., Tumskoy, V.E., Schirrmeister, L., 2022. Mammoth Fauna remains from late Pleistocene deposits of the Dmitry Laptev strait south Coast (northern Yakutia, Russia). Front. Earth Sci. 10, 757629 https://doi.org/10.3389/feart.2022.757629.

Melles, M., Brigham-Grette, J., Glushkova, O.Y., Minyuk, P.S., Nowaczyk, N.R., Hubberten, H.W., 2007. Sedimentary geochemistry of core PG1351 from Lake El'gygytgyn—a sensitive record of climate variability in the East Siberian Arctic during the past three glacial–interglacial cycles. J. Paleolimnol. 37, 89–104. https://doi.org/10.1007/s10933-006-9025-6.

Meyer, H., Dereviagin, A., Siegert, C., Schirrmeister, L., Hubberten, H.W., 2002. Palaeoclimate reconstruction on Big Lyakhovsky Island, North Siberia—hydrogen and oxygen isotopes in ice wedges. Permafr. Periglac. Process. 13 (2), 91–105. https://doi.org/10.1002/ppp.416.

Mochanov, Y.A., 1977. The Earliest Stages of Human Settlement in Northeast Asia. Nauka Publ, Novosibirsk (in Russ.).

Mochanov, Y.A., 1992. The Ancient Paleolithic Site of Diring and the Problem of a Nontropical Origin for Humankind. Nauka Publ, Novosibirsk (in Russ.).

Mochanov, Y.A., 1993. The most ancient Paleolithic of the Diring and the problem of a nontropical origin for humanity. Arctic Anthropol. 30, 22–53.

Mochanov, Y.A., Fedoseeva, S.A., 2007. Diring Yuriakh site of the most ancient Palaeolithic in Yakutia and the problem of extratropical ancestral home of humanity. Izvest. Lab. Drevn. Tekhnol. 1 (5), 75–99 (in Russ.).

Mochanov, Y.A., Fedoseeva, S.A., 2013a. Essays on the Preliterate History of Yakutia. Epohi Kamnya. Yakutsk (in Russ.).

Mochanov, Y.A., Fedoseeva, S.A., 2013b. Ocherki Dopis'mennoj Istorii Yakutii (Essays on the Preliterate History of Yakutia). Epohi kamnya, Yakutsk (in Russ.).

Murray, A.S., Wintle, A.G., 2000. Luminescence dating of quartz using an improved single-aliquot regenerative-dose protocol. Radiat. Meas. 32 (1), 57–73. https://doi.org/10.1016/S1350-4487(99)00253-X.

Murray, A.S., Wintle, A.G., 2003. The single aliquot regenerative dose protocol: potential for improvements in reliability. Radiat. Meas. 37, 377–381. https://doi.org/10.1016/S1350-4487(03)00053-2.

Murray, A.S., Marten, R., Johnston, A., Martin, P., 1987. Analysis for naturally occurring radionuclides at environmental concentrations by gamma spectrometry. J. Radioanal. Nucl. Chem. 115, 263–288. https://doi.org/10.1007/bf02037443.

Murray, A.S., Thomsen, K.J., Masuda, N., Buylaert, J.-P., Jain, M., 2012. Identifying well-bleached quartz using the different bleaching rates of quartz and feldspar luminescence signals. Radiat. Meas. 47 (9), 688–695. https://doi.org/10.1016/j.radmeas.2012.05.006.

Murray, A.S., Helsted, L.M., Autzen, M., Jain, M., Buylaert, J.-P., 2018. Measurement of natural radioactivity: calibration and performance of a high-resolution gamma spectrometry facility. Radiat. Meas. 120, 215–220. https://doi.org/10.1016/j.radmeas.2018.04.006.

Murray, A., Lee, J.A., Buylaert, J.-P., Gu'erin, G., Qin, J., Singhvi, A.K., Smedley, R., Thomsen, K.J., 2021. Optically stimulated luminescence dating using quartz. Nat. Rev. Meth. Primers. 1, 72. https://doi.org/10.1038/s43586-021-00068-5.

Nørgaard, J., Margold, M., Jansen, J.D., Kurbanov, R., Szuman, I., Andersen, J.L., Olsen, J., Knudsen, M.F., 2023. Absence of large-scale ice masses in central Northeast Siberia during the late Pleistocene. Geophys. Res. Lett. 50 (10), 1–10. https://doi.org/10.1029/2023GL103594.

Pitulko, V.V., Pavlova, E.Y., Nikolsky, P.A., Ivanova, V.V., 2012. Yanskaya site: material culture and symbolic activity of the Upper Paleolithic population of the Siberian Arctic. Rossiyskiy arheologicheskiy ezhegodnik. 2, 33–102 (in Russ.).

Pravkin, S.A., Bolshiyanov, D.Yu, Pomortsev, O.A., et al., 2018. Relief, structure and age of Quaternary sediments of the river valley. Lena in the Yakutsk bend. Vestnik Sankt-Peterburgskogo universiteta. Nauki o Zemle. 63 (2), 209–229 (in Russ.).

Prescott, J.R., Hutton, J.T., 1994. Cosmic ray contributions to dose rates for luminescence and ESR dating: large depths and long-term time variations. Radiat. Meas. 23, 497–500. https://doi.org/10.1016/1350-4487(94)90086-8.

Schirrmeister, L., Grosse, G., Schnelle, M., Fuchs, M., Krbetschek, M., Ulrich, M., Kunitsky, V., Grigoriev, M., Andreev, A., Kienast, F., Meyer, H., Babiy, O., Klimova, I., Bobrov, A., Wetterich, S., Schwamborn, G., 2011. Late quaternary paleoenvironmental records from the western Lena delta, arctic Siberia. Palaeogeogr. Palaeoclimatol. Palaeoecol. 299 (1–2), 175–196. https://doi.org/10.1016/j.palaeo.2010.10.045.

Schirrmeister, L., Froese, D., Tumskoy, V., Grosse, G., Wetterich, S., 2013. Yedoma: late Pleistocene ice-rich syngenetic permafrost of Beringia, 2nd edition Encyclopedia of Quaternary Science 542–552. https://doi.org/10.1016/B978-0-444-53643-3.00106-0.

Schirrmeister, L., Schwamborn, G., Overduin, P.P., Strauss, J., Fuchs, M.C., Grigoriev, M., et al., 2017. Yedoma ice complex of the buor Khaya Peninsula (southern Laptev Sea). Biogeosciences 14 (5), 1261–1283. https://doi.org/10.5194/bg-14-1261-2017.

Schwamborn, G., Schirrmeister, L., Mohammadi, A., Meyer, H., Kartoziia, A., Maggioni, F., Strauss, J., 2023. Fluvial and permafrost history of the lower Lena River, north-eastern Siberia, over late Quaternary time. Sedimentology 70 (1), 235–258. https://doi.org/10.1111/sed.13037.

Seppälä, M., 2012. Wind as a Geomorphic Agent in Cold Climates. Cambridge University Press.

Siegert, K., Stauch, G., Lehmkuhl, F., Sergeenko, A.I., Diekmann, B., Popp, S., Beloliubskii, I.N., 2007. Evolution of glaciations of the Verkhoyansk Range and its foothills in the Pleistocene: the results of new research. Regionalnaia Geologiya I Metallogeniya 30–31, 222–228 (in Russ.).

Stauch, G., Gualtieri, L., 2008. Late Quaternary glaciations in northeastern Russia. J. Quat. Sci. 23, 545–558. https://doi.org/10.1002/jqs.1211.

Stauch, G., Lehmkuhl, F., 2010. Quaternary glaciations in the Verkhoyansk mountains, Northeast Siberia. Quat. Res. No. 74, 145–155.

Strauss, J., Schirrmeister, L., Grosse, G., Fortier, D., Hugelius, G., Knoblauch, C., Romanovsky, V., Schädel, C., Schneider von Deimling, T., Schuur, E.A.G., Shmelev, D., Ulrich, M., Veremeeva, A., 2017. Deep Yedoma permafrost: a synthesis of depositional characteristics and carbon vulnerability. Earth Sci. Rev. No. 172, 75–86. https://doi.org/10.1016/j.earscirev.2017.07.007.

Tarasov, P., Müller, S., Zech, M., Andreeva, D., Diekmann, B., Leipe, C., 2013. Last glacial vegetation reconstructions in the extreme-continental eastern Asia: potentials of pollen and n-alkane biomarker analyses. Quat. Int. 290–291, 253–263. https://doi.org/10.1016/j.quaint.2012.04.007.

Thomsen, K.J., Murray, A.S., Jain, M., Bøtter-Jensen, L., 2008. Laboratory fading rates of various luminescence signals from feldspar-rich sediment extracts. Radiat. Meas. 43, 1474–1486. https://doi.org/10.1016/j.radmeas.2008.06.002.

Tukey, J.W., 1977. Exploratory Data Analysis. Addison Wesley, Reading, Mass.

Vasilieva, A.N., Murray, A.S., Taratunina, N.A., Buylaert, J.-P., Lytkin, V.M., Shaposhnikov, G.I., Stevense, T., Ujvari, G., Kurbanov, R.N., 2024. Dating the terraces of the Lena River (northeastern Siberia) using luminescence. Quat. Geochronol. (in press).

Velichko, A.A., Andreev, A.A., Klimanov, V.A., 1997. Climate and vegetation dynamics in the tundra and forest zone during the Late Glacial and Holocene. Quat. Int. 41/42, 71–96. https://doi.org/10.1016/S1040-6182(96)00039-0.

Velichko, A.A., Timireva, S.N., Kremenetski, K.V., MacDonald, G.M., Smith, L.C., 2011. West Siberian Plain as a late glacial desert. Quat. Int. 237 (1–2), 45–53. https://doi.org/10.1016/j.quaint.2011.01.013.

Waters, M.R., Forman, S.L., Pierson, J.M., 1997. Diring Yuriakh: a lower paleolithic site in central Siberia. Science 275, 1281–1284. https://doi.org/10.1126/science.275.5304.1281.

Waters, M.R., Forman, S.L., Pierson, J.M., 1999. Late Quaternary geology and geochronology of Diring Yuriakh, an early paleolithic site in central Siberia. Quat. Res. 51 (2), 195–211.

Wetterich, S., Tumskoy, V., Rudaya, N., Andreev, A.A., Opel, T., Meyer, H., Hüls, M., 2014. Ice complex formation in arctic east Siberia during the MIS3 interstadial. Quat. Sci. Rev. 84, 39–55. https://doi.org/10.1016/j.quascirev.2013.11.009.

Wolfe, S., Bond, J., Lamothe, M., 2011. Dune stabilization in central and southern yukon in relation to early Holocene environmental change, northwestern north America. Quat. Sci. Rev. 30 (3–4), 324–334. https://doi.org/10.1016/j.quascirev.2010.11.010.

Zaretskaya, N., Panin, A., Utkina, A., Baranov, D., 2024. Aeolian sedimentation in the Vychegda river valley, north-eastern Europe, during MIS 2–1. Quat. Int. 686–687, 83–98. https://doi.org/10.1016/j.quaint.2023.05.022.

Zech, W., Zech, R., Zech, M., Leiber, K., Dippold, M. Frechen, Bussert, R., Andreev, A., 2011. Obliquity forcing of Quaternary glaciation and environmental changes in NE Siberia. Quat. Int. 234 (1–2), 133–145. https://doi.org/10.1016/j.quaint.2010.04.016.